PAPER • **OPEN ACCESS**

A novel double chamber rotary sleeve air compressor -part II: friction losses model

To cite this article: Y A Alduqri *et al* 2020 *IOP Conf. Ser.: Mater. Sci. Eng.* **884** 012105

A novel double chamber rotary sleeve air compressor -part II: friction losses model

Y A Alduqri[1], H M Kamar[2], M N Musa [3], N B Kamsah [4], N R N Idris [5] and Gamal Alqaifi[6]

[1,2,3,4] School of Mechanical Engineering, Faculty of Engineering, Universiti Teknologi Malaysia, 81310 Johor, Malaysia.
[5] School of Electrical Engineering, Faculty of Engineering, Universiti Teknologi Malaysia, 81310, Johor Bahru, Johor, Malaysia.
[6] Faculty of Engineering, Civil Engineering Department, Universiti Putra Malaysia, 43400, Serdang, Seri Kembangan, Selangor, Malaysia.

E-mail: [1]yhy_ahmed@yahoo.com, *[2]haslinda@utm.my, [3]mdnor@ utm.my, [4]nazrikh@utm.my, [5]e-nrumzi@utm.my, [6]jamalalqaify@yahoo.com

Abstract. This paper presents the friction loss model of a novel double chamber rotary sleeve air compressor (DCRSC) concept. The compressor mechanism is similar to that of rotary compressor whereby the novelty transpires in the instalment of two rotating sleeves and a secured vane that has one end fixed to an outer sleeve and the other end to a rotor, respectively. This Part II of the paper series presents the friction losses analysis of the compressor. Thermodynamic and leakage losses models were respectively presented in Part I and Part III of this paper series. The primary aim of this paper is to formulate and analyse the friction loss model at the radial and axial contact regions of DCRSC at different rotational speed. The variations of the mechanical power and efficiency were evaluated based on the adiabatic, polytropic and isothermal thermodynamic principles as illustrated in Part I of this paper series. Considering the design simplicity of cylindrical shaped components, at maximum rotational speed of 1500 rpm, the DCRSC mechanical efficiencies are 72.43%, 66.2% and 59% when air undergoes adiabatic, polytropic and isothermal compression process, respectively. it is believed that the DCRSC is well suited for compressed air systems and air-conditioning applications.
Keywords: sleeve compressor, double-chamber, friction losses, modeling, simulation.

Nomenclatures

a	*Linear acceleration, m.s^{-1}*
e	*Inner sleeve offset distance from rotor center, m*
F_p	*Pressure force, N*
I	*Second moment of inertia, Kg.m^2*
L	*Length*, m
M	*Moment, N. m*
m	*Mass, Kg*
N	*Rotational Speed, rev.s^{-1}*
P	*Pressure*, bar
PW	*Power, W*
r	*Radius, m*
R	*Contact force, N*
t	*Thickness, m*

Subscripts

b	*End plate bearing*
c	*Compression*
d	*Discharge*
$diff$	*Due to pressure difference*
f	*Friction*
ic	*Inner chamber*
is	*Inner sleeve*
in	*Inner surface of the inner sleeve*
lo	*Lower bearing*
$mech$	*Mechanical*
oc	*Outer chamber*
os	*Outer sleeve*
ou	*Outer surface of the inner sleeve*
p	*Due to pressure*

Nomenclatures

v	*Velocity,* m.s^{-1}
W	*Work, J*
Γ	*Torque, N. m*
μ_f	*Coefficient of friction*
α	*Angular acceleration, rad. s^{-1}*
ω	*Angular velocity, rad. s^{-1}*
δ^o	*Assembly clearance gap, m*
β	*Rotor angle of rotation, rad*
ρ	*Density, Kg. m^{-3}*
θ	*Vane Angle to the inner sleeve center, rad*
η	*Efficiency*
ϕ	*Angle of the discharge groove, rad*

Subscripts

r	*Rotor*
s	*Suction*
tc	*Both chambers*
up	*Upper bearing*
v	*Vane*
vol	*Volumetric*
$adia$	*Adiabatic compression process*
$poly$	*Polytropic compression process*
$isoth$	*Isothermal compression process*
theo	*Theoretical results*

1. Introduction

A class of compressors that operate on the positive-displacement principle and employ rotary motion to transfer energy are described under the term rotary, which in short compresses gas [1, 2]. In general, there are four main types of rotary compressors: rotary vane compressors, scroll compressors, screw compressors and rolling piston rotary compressors that are used in a variety of applications. Compared with other rotary types, the scroll type compressors show higher performance and smoother operation, yet have complex structure and is difficult to manufacture [3-5].

It all started with the concept development of single-vane compressor which is featured with an eccentric sleeve and two compression chambers [6]. The multi-vane rotary compressor was developed by [7]. Then a study developed what's called a vacuum rotary compressor [8]. In his compressor, a reduction of frictional losses and wear were significantly highlighted whereby lighter materials were used for the parts that undergone motion, which effectively decrease the friction force between the cylinder wall and the vane tip. To moreover decrease the vane tip load, a research introduced the concept of the multi-sliding vane compressor [9]. A dual sliding vane rotary compressor was developed to increase the pressure ratio, however such improvement lead to high friction losses due to the sliding vanes [10]. A numerical analysis of friction force and wear of rotary vane compressor was conducted by [11] . Furthermore, a study investigated the friction force and the overcoming wear between vane and rotor Surface [12]. A reduction of friction was achieved by reducing the speed of rotation of the rotary vane compressor. The introduction of dual-chamber sliding vane rotary compressor was implemented whereby more fluid quantity is charged and compressed with a better mechanical efficiency than that of a single-chamber sliding vane rotary compressor [13]. Improvements methods have been implemented to increase the durability and efficiency of the rotary compressor. For instant, the coating technology is used to decrease the friction losses to achieve higher mechanical efficiency, leakage losses and lubricant studies to achieve higher cooling capacity, and parametric studies for higher performance [14].

These rotary type compressors have higher efficiency and reliability, are also less subjected to mechanical vibration and, for a given volumetric capacity, are usually smaller, light compacted than their reciprocating compressor [15-17]. Various types of rotary compressors are able to perform well in both automotive and residential applications, however, they still have lower efficiency when compared to the scroll compressor. The critical factors affecting the overall efficiency of the rotary compressors are mainly the friction and internal leakage losses. In most of the existing rotary vane compressors, the sliding vane usually possesses high friction at high relative velocity which limits their performance [18-20].

As reviewed by studies [21-24] , rotary types compressors are subjected to high friction when running at a higher speed which in return bring out poorer and limited performance. The friction losses are considered amongst the significant factors impacting rotary compressor performance. A new rotary compressor (Two- sleeve rotary compressor) was introduced to minimize the friction losses amongst other hinderances such as leakage losses [25]. Based on the sleeve rotating mechanism introduced by the study [25], the double chamber rotating sleeve compressor was developed. The proposed double chamber rotary sleeve compressor introduces non-sliding vanes and rotating sleeves concept, which

minimizes the relative velocity between the rotating components and eliminate friction at the vane tip thus improving the mechanical efficiency. The configurations and compression mechanism of the DCRSC are detailed in Part I of this paper series [26].

2. Mathematical friction losses model of the DCRSC

As illustrated on Figure 1a, there are mainly three radial regions of friction in the double chamber rotary sleeve compressor. The radial locations are, at the inner sleeve tip and vane contact, at the radial contact between the inner sleeve and the rotor, and at the radial contact between the inner and outer sleeves [26]. As shown in Figure 2b, there are mainly eight axial regions of friction in this compressor. The axial contact regions contacts are, two regions at the vane ends on the two end plate bearings, two regions at the inner sleeve path on the two end plate bearings, two regions at the outer sleeve ends on the two end plate bearings, two regions at the rotor ends on the two end plate bearings. Since the compressor is placed horizontally, axial contacts will have less friction when compared to the radial contact due to gravity is perpendicular to the radial direction. Outer sleeve and rotor axial contacts where not used on calculating the friction losses because they have bearing and lubrication on all of the contact region and gravity is perpendicular to these regions so we expect minimum friction at these regions and where ignored during the analysis. The working compression cycle for a complete revolution is presented in Part I of this paper series [26].

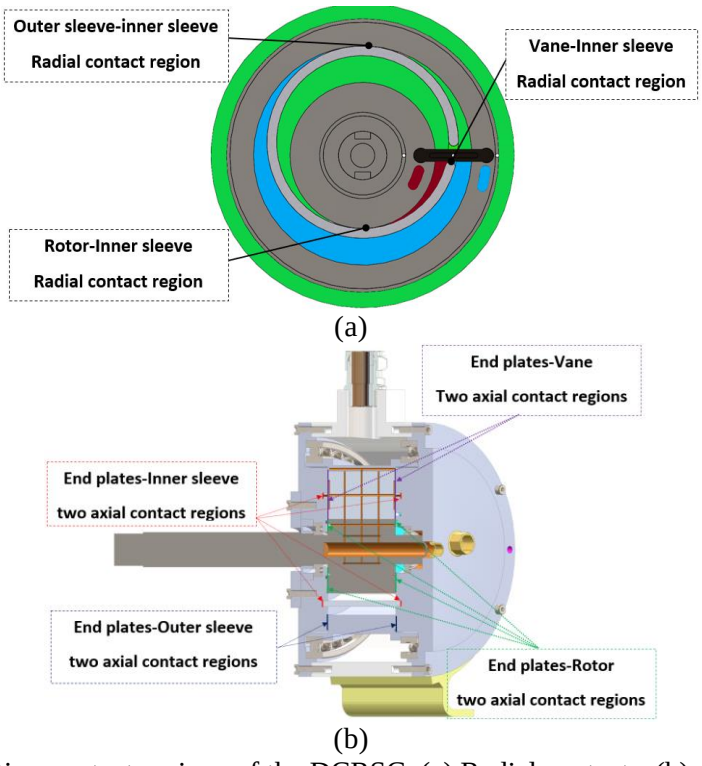

Figure 1. Friction contact regions of the DCRSC, (a) Radial contacts, (b) Axial contacts.

The air pressure inside the compression chambers were used in the friction loss model based on the three thermodynamic compression principles as detailed in Part I of this paper series [26]. The inner sleeve inertia force, contact and reaction forces are illustrated in Figure 2. In this analysis, it is assumed that the pressure force due to the pressure difference between the outer chamber and the inner chamber acts as a single dynamic force on the inner sleeve, since the rotating mechanism of the compressor is entirely dependent on the sliding motion of the inner sleeve.

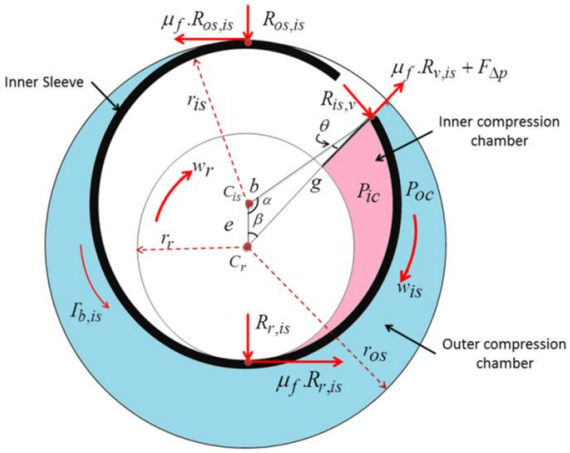

Figure 2. Forces acting on the inner-sleeve of DCRSC.

From Figure 3, the force analysis begins by taking the moment about the centre of the inner sleeve (equation 1), and the rotor centre (equation 1), and by taking the radial forces (equation 3) and tangential forces (equation 4) acting on the inner sleeve.

$$\sum M_{C_{is}}: \begin{bmatrix} (eg - \cos\beta - \mu_f \sin\beta) \\ -\mu_f(r_{os} - e) \\ -\mu_f(r_r + e) \\ -1 \end{bmatrix} \times \begin{bmatrix} R_{is,v} \\ R_{os,is} \\ R_{r,is} \\ \Gamma_{is,b} \end{bmatrix} = [I_{is}\sigma_{is}] \tag{1}$$

Where,

$$F_{\Delta p} = \frac{P_{ic}}{A_{is,in}} - \frac{P_{oc}}{A_{is,on}}, \quad g = e\cos\beta_i + r_{is}\sqrt{\left(r_{is}^2 - e^2\left(\frac{1}{2}\cos 2\beta\right)\right)},$$

$$\theta = \sin^{-1}\left(\frac{e}{r_{is}}\sin\beta\right).$$

$$\sum M_{C_r}: \begin{bmatrix} g \\ -\mu_f r_{os} \\ -\mu_f r_r \\ 0 \end{bmatrix} \times \begin{bmatrix} R_{is,v} \\ R_{os,is} \\ R_{r,is} \\ \Gamma_{is,b} \end{bmatrix} = [I_r\sigma_r - gF_{\Delta p}\sin\theta] \tag{2}$$

The analysis continues by taking all contact and frictional forces acting on the inner sleeve in the radial and tangential directions as described in Equations (3) and (4). The force equation is derived using the second law of Newton for a curvilinear motion and can be formulated as follows,

$$F_{radial}: \begin{bmatrix} -\sin\theta - \mu_f\cos\theta \\ 1 \\ -1 \\ 0 \end{bmatrix} \times \begin{bmatrix} R_{is,v} \\ R_{os,is} \\ R_{r,is} \\ \Gamma_{is,b} \end{bmatrix} = [m_{is}(a_{is} - r_{is}\omega_{is}^2) + F_{\Delta p}] \tag{3}$$

$$F_{tangential}: \begin{bmatrix} \cos\theta - \mu_f\sin\theta \\ -\mu_f \\ -\mu_f \\ 0 \end{bmatrix} \times \begin{bmatrix} R_{is,v} \\ R_{os,is} \\ R_{r,is} \\ \Gamma_{is,b} \end{bmatrix} = [m_{is}(r_{is}\sigma_{is} - 2v_{is}\omega_{is})] \tag{4}$$

The four unknown forces can be solved simultaneously using 4th order Runge-Kutta numerical integration by a MATLAB program, combining all Equations (1) to (4) in matrix form. An iteration of the angle β of rotation can be conducted to find the variation of all unknown forces for one complete cycle.

$$\begin{bmatrix} (eg - \cos\beta - \mu_f \sin\beta) & -\mu_f(r_{os} - e) & -\mu_f(r_r + e) & -1 \\ g & -\mu_f r_{os} & -\mu_f r_r & 0 \\ -\sin\theta - \mu_f \cos\theta & 1 & -1 & 0 \\ \cos\theta - \mu_f \sin\theta & -\mu_f & -\mu_f & 0 \end{bmatrix} \times \begin{bmatrix} R_{is,iv} \\ R_{os,is} \\ R_{r,is} \\ I_{is,b} \end{bmatrix} = \begin{bmatrix} I_{is}\sigma_{is} \\ I_r\sigma_r - gF_{\Delta p}\sin\theta \\ m_{is}(a_{is} - r_{is}\omega_{is}^2) + F_{\Delta p} \\ m_{is}(r_{is}\sigma_{is} - 2v_{is}\omega_{is}) \end{bmatrix} \quad (5)$$

Concerning **Error! Reference source not found.**, all contact forces will generate friction power. The friction power can be calculated using the following relations:

$$PW_f = \left[\left(\mu_f R_{is,v} |v_v - v_{is}|\right)_v + \left(\mu_f R_{is,os} |v_{os} - v_{is}|\right)_{os} + \left(\mu_f R_{is,r} |v_r - v_{is}|\right)_r + \left(\mu_f T_{is,b}(\omega_{is})\right)_b \right] \quad (6)$$

The mechanical power of the DCRSC can be expressed as:

$$PW_{mech} = PW_c + PW_f \quad (7)$$

Where the compression power (PW_c) is the total hydraulic power of the inner chamber and outer chamber required to compress the air. The compression power at adiabatic, polytropic and isothermal compression process is presented in Part I of this paper series[26].

$$\eta_{mech} = (PW_c / PW_{mech}) \times 100\% \quad (8)$$

3. Main results and discussion

The mathematical model has been used to theoretically predict the compressor mechanical performance with the aid of computing effort. The theoretical analysis can be served as the tool for parametric studies and optimization for a better compressor design. The DCRSC operation parameters and main dimensions are detailed in Part I of this paper series.

3.1 Friction losses analysis: pressure and contact forces

Figure 3a ,3b and 4c show the variation of the air pressure forces acting on the inner sleeve for two complete working cycles under adiabatic, polytropic and isothermal compression model, respectively. The analysis of air pressure inside each chamber is presented in Part I of this paper series. As shown in Figure 3, the pressure forces acting on the inner sleeve profile increases during compression and reaches its peak value when the air starts to discharge for each perspective compression chamber. Figure 3d, shows the total pressure difference acting on the inner sleeve, it can be seen the forces acting on the inner sleeve changes direction based on what of the two compression chambers has the higher pressure during the rotational cycle. From Figure 4d, the adiabatic compression process exerts more pressure force on the inner sleeve and the isothermal compression process has smaller pressure force due to the high-pressure ratio of the adiabatic compression.

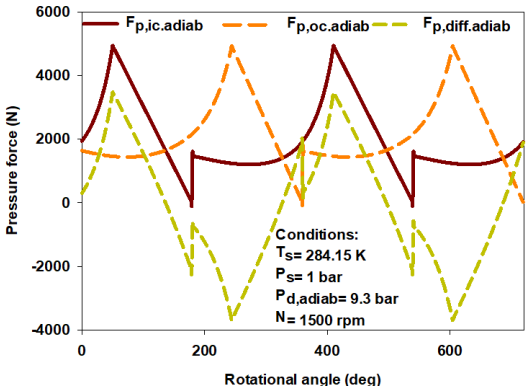

(a)

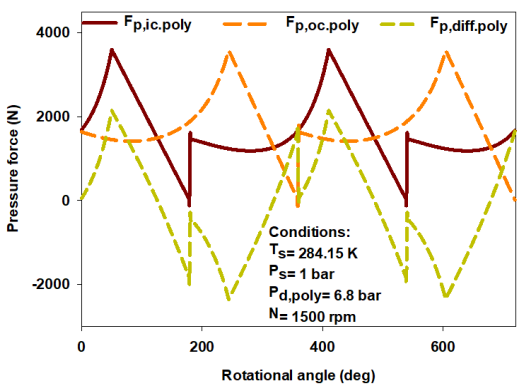

(b)

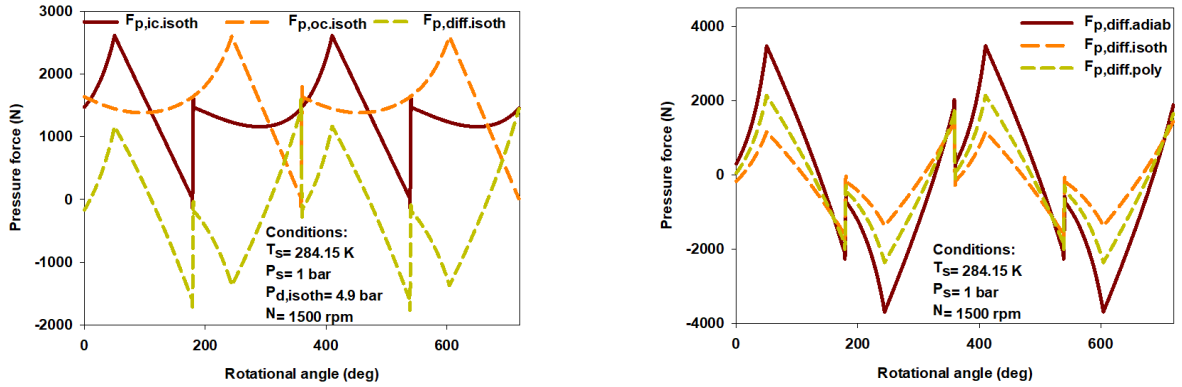

(c) (d)

Figure 3. The profile of pressure forces acting on the inner sleeve for two rotational cycle due to (a) adiabatic compression process, (b) polytropic compression process, (c) isothermal compression process, (d) Overall pressure forces profile.

Figure 4 shows variation of the generated friction forces between the inner sleeve and each of the vane, outer sleeve, rotor, end plate bearings during the two complete rotational cycles. During compression stage, the inner sleeve and vane contact force average is about 1110 N which contributes to 32.6% of the total generated friction forces, the inner sleeve and outer sleeve contact will generate an average friction force of 695N or 20.4%of the total friction, the inner sleeve and rotor contact will produce an average 1157N friction force which contributes highest percentage at 34% of the total friction, while the inner sleeve and end plate bearings will only generate an average friction force of 442N or 13% of the total friction.as shown in figure 6d, the maximum generated friction forces will be at its peak when the compressed air start to discharge from each of the inner and outer compression chambers.

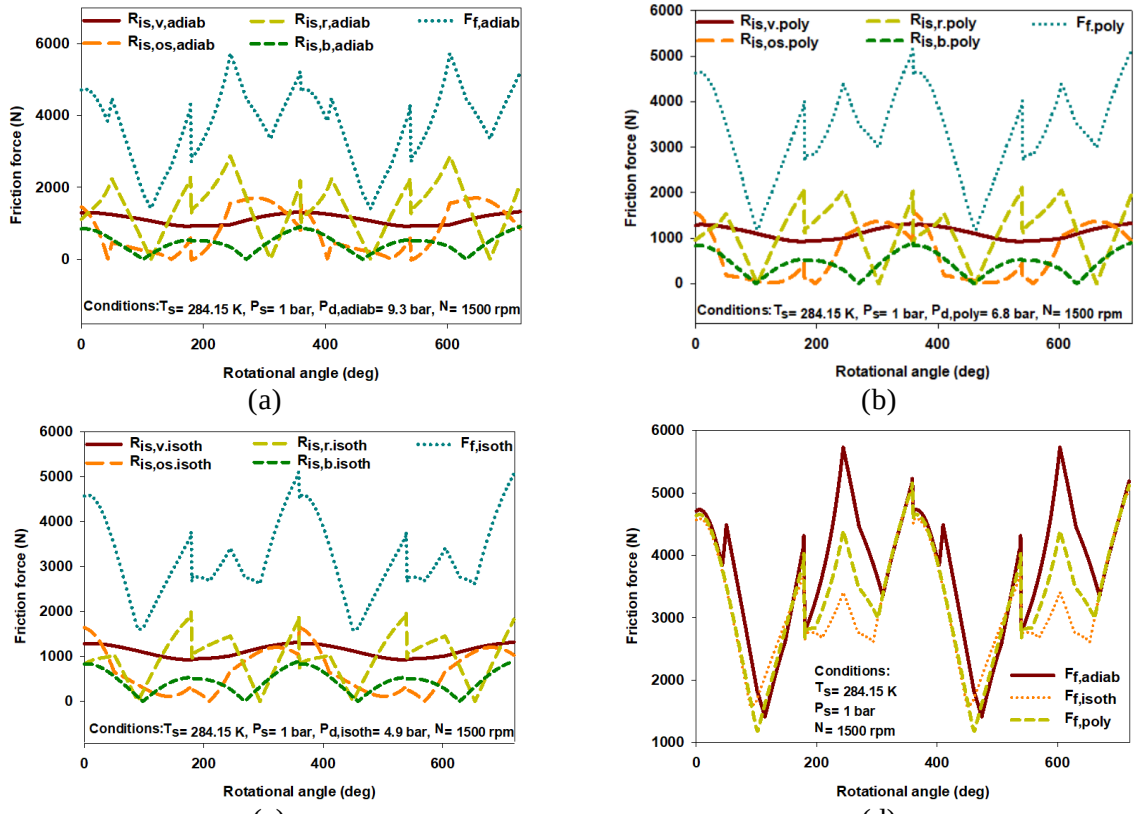

(a) (b)

(c) (d)

Figure 4. The profile of friction forces during two rotational cycle for (a) adiabatic compression, (b) polytropic compression, (c) isothermal compression, (d) Total friction forces.

3.2 Mechanical power and efficiency

Figure 5 shows the mechanical power losses due to friction forces generated between the inner sleeve and each of the vane, outer sleeve, rotor and end plate bearings at maximum rotational speed of 1500 rpm. The value of the dynamic coefficient of friction is assumed as 0.09. Experimental studies of sliding stainless steel components show the dynamic coefficient of friction is around 0.05~0.09. The friction power graph on figure 6d, shows a peak friction of 868 W at the end of the outer chamber compression. Based on the current design[26], the inner chamber compression begins after 180° from the beginning of the outer chamber compression, and since double compression chambers are acting on the inner sleeve continuously, double chamber rotary air compressor frictional power is expected to be lower than the friction power of a single acting compression chamber compressor.

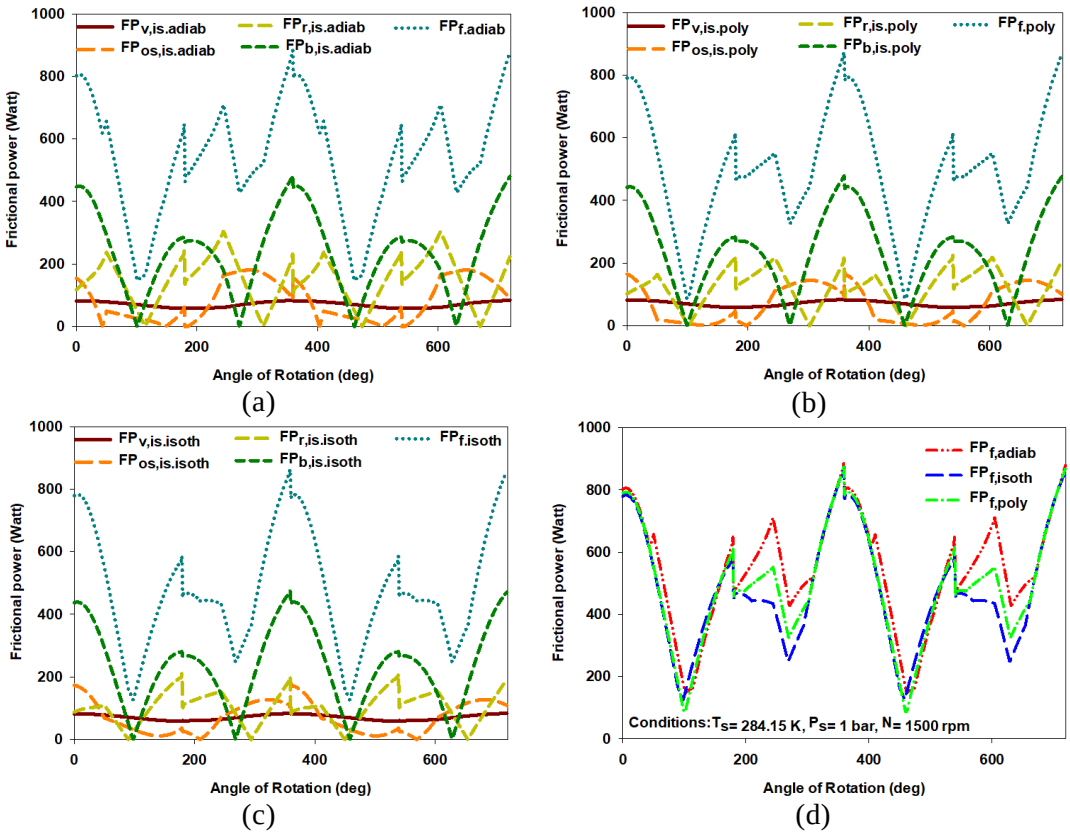

Figure 5. The profile of friction power during two rotational cycle for (a) adiabatic compression process, (b) polytropic compression process, (c) isothermal compression process, (d) Total friction power.

Figure 6 shows the total friction power of the compressor at different rotational speed ranging from 500 to 1500 rpm. The figure indicates the increase of rotational speed will rapidly increase the friction losses because the higher the rotational speed the lower metal to metal clearance and that leads to higher friction.

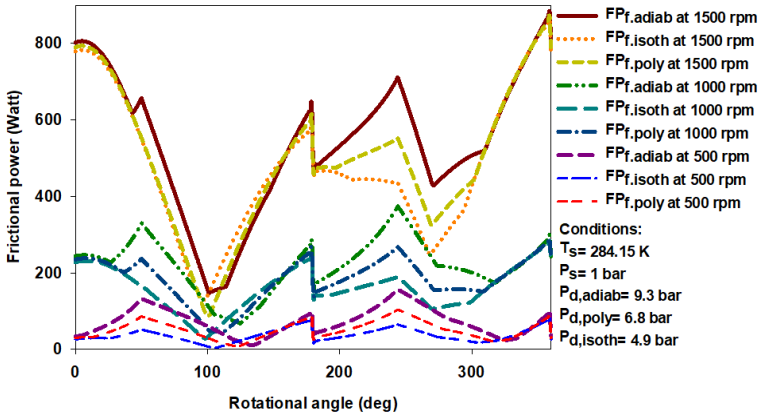

Figure 6. DCRSC frictional power for various rotational angles at different rotational speed.

Figure 7 show the mechanical power and mechanical efficiency of the DCRSC at different rotational speed. At maximum rotational speed of 1500 rpm, the compressor requires an input power of 1876W, 1458W, 1157W to compress the air from 1 bar to 9.3 bar, 6.8 bar, 4.9 bar, respectively, when the compressor undergoes adiabatic, polytopic and isothermal compression process. From figure 7b, the compressor mechanical efficiency is 71.3%, 66.2%, 59% when the rotational speed for adiabatic, polytropic and isothermal compression process. The compressor will have the highest mechanical efficiency when the air is compressed close to the ideal reversable adiabatic compression process. Figure 7b shows the compressor will most likely undergo an isothermal compression at low rotational speed up to 400 rpm where the friction is low and heat build-up is very low, however the leakage flow rate will be higher at lower speed as presented in Part III of this paper series [27].

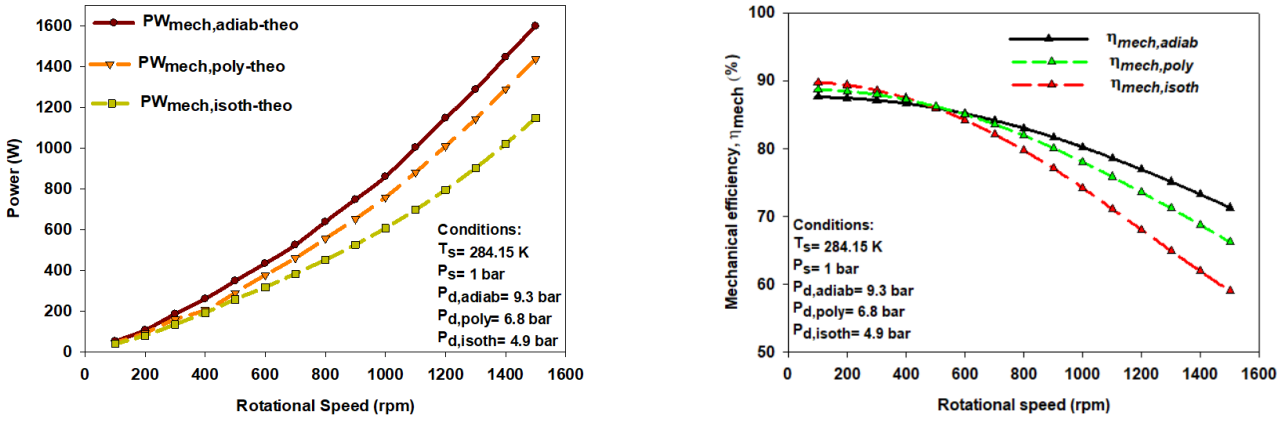

(a) (b)

Figure 7. The variation of the mechanical power and efficiency of the DCRSC for the adiabatic, polytropic and isothermal compression process at different rotational speed (a) mechanical power, (b) mechanical efficiency.

4. Conclusion

In this paper, friction losses of a novel double-chamber rotary sleeve compressor have been theoretically modelled and analysed. The compressor's uniqueness is with the introduction of the two eccentric sleeves and end fixed vane that create two different compression chambers. The preliminary thermodynamic analysis of the DCRSC is presented in Part I of this paper series. The friction model focuses mainly on the contact and pressure forces acting on the inner sleeve. It has been found the metal to metal contacts between the inner sleeve and each of the vane, outer sleeve, rotor, end plate bearings contribute to 32.6%, 20.4%, 34%, 12% of the total friction produced during compression, respectively. For adiabatic, polytropic, isothermal compression process, the DCRSC has respectively a mechanical efficiency of 72.43%, 66.2% and 59% at maximum rotational speed of 1500 rpm. Although, the new compressor has effectively minimized the frictional loss at the vane which poses

the highest friction on the existing rotary vane compressors, there is a room for further reduction of the friction losses by increasing the assembly clearances at the contact points or surfaces, without significantly affecting the volumetric efficiency of the compressor. For further improvement in the efficiency of the proposed compressor, material selection and suitable assembly clearances need to be studied with bearing in mind on the reduction of metal to metal contact and the implementation of a good lubricating system.

Acknowledgments
The authors are grateful to the Universiti Teknologi Malaysia and *Ministry of Science*, Technology and Innovation, for providing the funding for this study, under the vote number 20H44 and R.J130000.7909.4S086, respectively. The financial supports are managed by the Research Management Centre (RMC), Universiti Teknologi Malaysia.

References
[1] Bloch, H.P. and A. Godse, Compressors and Modern Process Applications. 2006: Wiley.
[2] Abagnale, C., et al., Ideal Specific Work of Rotary Compressors: A New Approach. Energy Procedia, 2016. 101: p. 710-717.
[3] Akazawa, T., et al., Development of a high-performance scroll compressor for automotive air conditioners. 1996.
[4] Hu, X., et al., Theoretical study on frictional losses of a novel automotive swing vane compressor. International Journal of Refrigeration, 2013. 36(3): p. 758-767.
[5] Yi, F. and Y. Qian, Developing a compact automotive scroll compressor. 2008.
[6] Gillespie, J.E., Improvement in rotary pumps. 1873, Google Patents.
[7] Walter, J.P., Rotary Pump, in U.S. Patent. 1923, US1444269 A.
[8] Camilo, V.N., Rotary vacuum and compression pump. 1954, Google Patents.
[9] Adalbert, G., J. Hess, and E. Linder, Pressure-sealed compressor. 1974, Google Patents.
[10] Shouman, A., et al., Performance evaluation of a novel dual vane rotary compressor. IOP Conference Series: Materials Science and Engineering, 2017. 232(1): p. 012060.
[11] Hervas, E., et al., Numerical Analysis of Friction power and Wear of Vane in Rotary Compressor. 2018.
[12] Rukanskis, M., Vane Friction and Wear Influence on Rotary Vane Compressor Efficiency and Operation: Research and Analysis Review. Agricultural Engineering, 2017. 49: p. 1-12.
[13] Adalbert, G. and T. Vysiotis, Vane compressor, particularly a cooling medium compressor for use in air-conditioning equipment of a vehicle. 1985, Google Patents.
[14] Yang, J.-S., et al., A sensitivity study of size parameters in a twin-type rolling piston compressor. International journal of refrigeration, 2013. 36(3): p. 786-794.
[15] Chang, K., A Theoretical and Experimental Study of An Oil-Flooded Rotary Sliding Vane Compressor (Vol. 1 & 2). 1983, Ph. D Thesis, University Of Strathclyde.
[16] Barreto, A., J. Kopelowicz, and J.A. Parise, Simulation of An Innovative Rotary Compressor With Variable Speed Displacers. 2004.
[17] Diniz, M.C. and C.J. Deschamps, Comparative Analysis of Two Types of Positive Displacement Compressors for Air Conditioning Applications. 2016.
[18] Matsuzaka, T. and S. Nagatomo, Rolling piston type rotary compressor performance analysis. 1982.
[19] Ozu, M. and T. Itami, Efficiency analysis of power consumption in small hermetic refrigerant rotary compressors. International Journal of Refrigeration, 1981. 4(5): p. 265-270.
[20] Yanagisawa, T. and T. Shimizu, Friction losses in rolling piston type rotary compressors. III. International journal of refrigeration, 1985. 8(3): p. 159-165.
[21] Aradau, D. and L. Costiuc, Friction power in sliding vane type rotary compressors. 1996.
[22] Kruse, H., Experimental investigations on rotary vane compressors. 1980.

[23] Bei, G. and L. Liansheng, Study of dynamic characteristics of cylinder profile of rotary vane compressor for automotive air conditioner. Refrigeration Journal, 2003. 2: p. 010.
[24] Sarip, M. and A. Rahim, Development And Analysis a New Integrated Motor Rotary Vane Compressor, in Faculty of Mechanical Engineering. 2016, Universiti Teknologi Malaysia.
[25] Musa, M.N., Two Sleeve Rotary Compressor, in MY Patent. 2003, MY130648A.
[26] Alduqri Y.A, K.H.M., Musa M.N, Kamsah N, Idris R, Gamal Alqaifi, A novel double chamber rotary sleeve air compressor part I: design and thermodynamic model. Sustainable and Integrated Engineering international conference 2019. in press.
[27] Alduqri Y.A, K.H.M., Musa M.N, Kamsah N, Idris R, Gamal Alqaifi, A novel double chamber rotary sleeve air compressor part III: leakage losses model. Sustainable and Integrated Engineering international conference 2019. in press